THE ASTROPHYSICAL JOURNAL, 412:L47–L50, 1993 August 1

COSMIC BACKGROUND RADIATION ANISOTROPY AT DEGREE ANGULAR SCALES: FURTHER RESULTS FROM THE SOUTH POLE

JEFFREY SCHUSTER,[1] TODD GAIER, JOSHUA GUNDERSEN,[2] PETER MEINHOLD,[2] TIMOTHY KOCH, MICHAEL SEIFFERT, CARLOS ALEXANDRE WUENSCHE,[3] AND PHILIP LUBIN[2]
Department of Physics, University of California Santa Barbara, Santa Barbara, CA 93106-9530
Received 1993 March 26; accepted 1993 May 13

ABSTRACT

We report further results from the University of California at Santa Barbara program to measure anisotropy in the cosmic background radiation at angular scales near 1°, an angular range corresponding to the largest scales where structure is observed. A 30 GHz high electron mobility transistor amplifier based detector was coupled to the Advanced Cosmic Microwave Explorer, a 1 m off axis Gregorian telescope. We present data that represent 64 of the total of 500 hr acquired with this system during the 1990–1991 season. The data have a statistical error of 13.5 μK pixel^{-1}. These are the smallest error bars of any data set of this type published to date. The data contain a significant signal with a maximum likelihood $\Delta T/T \approx 1 \times 10^{-5}$, under the assumption of a Gaussian sky autocorrelation function at a coherence angle of 1°.5. The spectrum of the signal seen in slightly less than 2 σ away from the thermal spectrum expected of primordial fluctuations in the cosmic background radiation. If the source of the fluctuations is primordial, then the data are consistent with cold dark matter scenarios when normalized to the large-scale anisotropy observed by *COBE*, while if the origin of the signal is foreground emission or another form of contaminant then the data are marginally inconsistent with standard cold dark matter models. In either case, the data are sufficiently sensitive to provide a crucial test of many models.

Subject headings: cosmology: cosmic microwave background — large-scale structure of universe

1. INTRODUCTION

The cosmic background radiation (CBR) is one of the best probes of the universe at $z \geq 1100$. Gravitational potential differences between regions on the surface of last scattering separated by more than $\sim 1°$ give rise to temperature fluctuations in the CBR (Sachs & Wolfe 1967). Smaller angular scales are inside the Hubble radius at decoupling, and thus are causally connected. This allows for coherent velocity flows which give larger CBR fluctuations than those expected at larger angles. Below 10′ the amplitude is damped due to the thickness of the surface of last scattering (for example, see Bond et al. 1991, hereafter BELM; or Vittorio & Silk 1992). Published treatments of CBR anisotropy often describe the theoretically expected CBR fluctuation distribution using a sky correlation function:

$$C(\Theta) = \left\langle \frac{\Delta T}{T}(\hat{q}_1) \frac{\Delta T}{T}(\hat{q}_2) \right\rangle , \quad (1)$$

where $\cos(\Theta) = \hat{q}_1 \cdot \hat{q}_2$ and $\Delta T/T(\hat{q}_i)$ is the CBR temperature fluctuation in the direction of the unit vector $\hat{q}_i$ (cf., Wilson & Silk 1980 or Bond & Efstathiou 1987). While measurements at a single angular scale are not sufficient to constrain theories, the sky correlation function can be normalized using other data, for example the galaxy-galaxy correlation function (cf. Wright et al. 1992 or BELM), large-scale velocity fields (cf. Gorski 1992), or to the recent *COBE* DMR detection (Smoot et al. 1992).

[1] Present mailing address: Department of Physics, University of California Berkeley, Berkeley, CA 94720.
[2] Also Center for Particle Astrophysics, Berkeley, CA 94720.
[3] Also the Instituto Nacional de Pesquisas Espaciais—INPE/MCT, Departamento de Astrofísica, São José dos Campos, SP, Brazil 12200.

2. THE INSTRUMENT

The University of California at Santa Barbara Advanced Cosmic Microwave Explorer (ACME) is a 1 m off-axis Gregorian telescope and stabilized platform used in a series of CBR measurements in both balloon-borne and ground-based configurations. We used the imaging capabilities inherent in a Gregorian design to obtain a 1°.5 full width at half-maximum power response (FWHM) beam with very low side lobes. The ellipsoidal secondary oscillated sinusoidally about the feed symmetry axis to give a peak to peak throw of the beam on the sky of 3°. This resulted in maximum sensitivity to sky temperature differences separated by 2°.1. The relationship between the sky temperature and our quoted ΔT's is identical to that in BELM.

We used a cryogenic high electron mobility transistor (HEMT) amplifier, operating at a center frequency of 30 GHz and having a 30% bandwidth (Pospieszalski, Gallego, & Lakatosh 1990). This wide band, coupled with the very low noise temperature of 30 K, gives a theoretical noise (with no sky contribution) of 0.6 mK s^{-1}. We achieved a noise of 1 mK s^{-1} on the sky, including atmospheric noise. The full band was divided into 4 subbands of equal (2.5 GHz) widths. This allowed for the widest effective bandwidth and also afforded some spectral discrimination to distinguish foreground sources. The four signals were detected with square-law diodes, synchronously demodulated, and integrated for 1.25 s.

To test system calibration and pointing, data on the moon, the Large Magellanic Cloud and the Galactic plane were taken. Daily calibrations were obtained by inserting an ambient temperature blackbody target into the beam, and the system calibration was found to be stable to $\pm 3\%$ for the duration of the data gathering period.

A detailed discussion of the ACME telescope is given in Meinhold et al. (1993) and many details pertaining to this work were previously described in Gaier et al. (1992).

3. THE SITE

The Amundsen-Scott South Pole station is one of the best millimeter-wave observing sites currently available in the world. Precipitable water was below 1 mm for most of the data taking period (Schuster et al. 1993). This offered many sections of continuous high-stability data that were longer than 24 hr.

Observing at a pole also affords a unique geometrical advantage. All data taken at constant elevation, as required by the need to observe through constant column densities of air, are also taken at constant declination. Additionally, the Sun remains approximately fixed with respect to the instrument. These facts facilitate extremely long integrations by reducing the normal problems of diurnal variations and eliminating beam smearing due to sky rotation (for a description of this effect, see Readhead et al. 1989). Observing continuously over many days allowed for very sensitive tests of potential systematic signals that repeated in azimuth, such as side lobe contamination or systematic effects from the tracking system.

4. OBSERVATION STRATEGY

The scan strategy was similar to that used in previous observations (e.g., Meinhold & Lubin 1991) and is described in Gaier et al. (1992). We chose the target coordinates by examining the 408 MHz map of Haslam et al. and the 100 μm *IRAS* map for a region of the sky relatively free from synchrotron and dust emission. In this region we acquired 500 hr of data. The data are separated into 8 data sets at six separate elevations and centered on three distinct right ascensions. Each of these data sets consists of a set of target points at constant elevation, separated by 2°.1. The data presented here consist of 15 sky temperature differences. All are at declination $-63°$, and the center of the data set is at 2^h right ascension.

For this data set, a single scan was acquired by stepping consecutively between the 15 target points, integrating for 25 s each. The following scan moves in the reverse direction. In this way 526 scans were performed over a period of 64 hr starting at 14:46 UT on 1991 January 5.

5. DATA REDUCTION

We removed 37% of the data, including measurements made while the telescope was not pointed at the desired right ascension and declination, data taken during calibrations, errors in the beam modulation, and other errors. The data were then filtered by removing an offset and a gradient in time across each scan. An rms and average were calculated for each 25 s integration. If the χ^2 of these averages for a complete scan exceeded the 99th percentile expected based on the calculated rms, we rejected the scan. This resulted in removal of 5%–10% of the scans, depending on the band. This criterion was used because any single scan with such a large signal could not be due to CBR fluctuations and must be contaminated. This is confirmed by the amplitude of the signal in the final data set. However, the final result did not depend strongly on how tightly this cut was applied. For comparison, we also reduced the data by removing single scans that had a large rms, as has been done in previous work (Gaier et al. 1992). The results were consistent with the previous method. The averages, weighted by their individual variances, were added together.

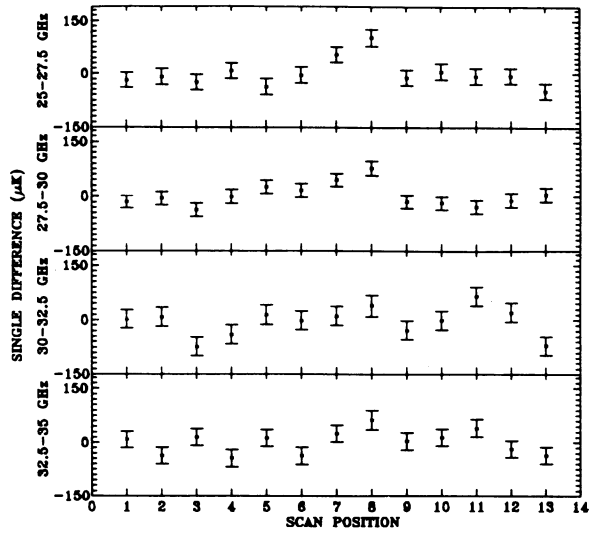

Fig. 1.—Sky temperature differences for points separated by 2°.1. (*a*) Data from the individual frequency bands. (*b*) Full band data.

The results at this point are shown in Figure 1*a*. Data from the four channels were combined to create the final data set shown in Figure 1*b*. These data are tabulated in Table 1. In addition, Monte Carlo data sets were analyzed in an identical fashion to verify that the final data points were unbiased. The data were also reduced in azimuthal and Sun-centered coordinates to check for systematic effects. By analyzing other data taken at angles closer to the Sun, we found those target points closer than 65° to the Sun might have a significant signal from the Sun, and for this reason we used only the first 13 points of the scan. Further details of various tests of systematics will be included in an upcoming publication.

6. ANALYSIS AND RESULTS

To put limits on theoretical models, we use a Bayesian analysis with a uniform prior. This analysis assumes the probability distribution of the sky amplitude given the data is the likelihood:

$$\mathcal{L} = (2\pi)^{-N/2} |M|^{-1/2} \exp\left(-\tfrac{1}{2} D_i M_{ij}^{-1} D_j\right), \qquad (2)$$

where the D_i are suitably defined final data points and the information about the model sky, instrument, and scan strategy are contained in the covariance matrix, M. Linear gradient and offset subtraction were accounted for by using the amplitudes of the best-fit Legendre polynomials, P_2 through P_{12}, for the D_i. The amplitudes of P_0 and P_1, the constant and linear functions, were not used because they correspond to the functions that were fitted out in the data reduction process.

For comparison to other results, we chose to compute limits using a Gaussian sky correlation function:

$$C(\Theta) = C_0 \exp\left(-\frac{\Theta^2}{2\Theta_c^2}\right), \qquad (3)$$

where Θ_c is the sky coherence angle, and $C_0^{1/2}$ is the sky rms. Figure 2 shows the likelihood function at $\Theta_c = 1°.5$, and Figure 3 shows the limits and maximum likelihood detection as a function of Θ_c. For the rest of this work, all stated limits and detections are in the context of a Gaussian correlated sky with Gaussian statistics. Because the beam is assumed to be a

TABLE 1

$\delta = -63$ DATA SET

Scan Position	R.A.	Channel 1 Average (μK)	Channel 1 rms (μK)	Channel 2 Average (μK)	Channel 2 rms (μK)	Channel 3 Average (μK)	Channel 3 rms (μK)	Channel 4 Average (μK)	Channel 4 rms (μK)	Full Band Average (μK)	Full Band rms (μK)
1	4h16	−19.4	21.1	−15.2	17.4	2.6	24.9	8.5	22.9	−16.2	12.6
2	3.85	−8.8	22.3	−5.6	18.1	9.0	26.0	−36.1	24.0	−0.8	13.4
3	3.54	−24.1	22.0	−37.1	18.4	−73.2	25.9	16.2	23.7	−19.8	13.3
4	3.23	8.4	21.9	−0.8	18.2	−39.7	26.5	−43.4	24.1	−10.6	13.5
5	2.93	−36.3	22.7	25.5	18.6	14.0	26.0	12.5	23.9	−9.8	13.5
6	2.62	−4.5	22.3	15.2	18.5	−1.4	26.2	−36.9	23.8	5.0	13.6
7	2.31	53.4	22.3	44.3	18.4	11.1	26.2	25.1	23.4	38.5	13.3
8	2.00	101.0	24.5	76.6	20.2	40.0	29.2	62.0	26.8	53.1	14.5
9	1.69	−12.0	22.1	−14.1	18.3	−27.4	26.2	3.5	23.9	−9.0	13.4
10	1.38	5.2	22.2	−17.2	18.3	−1.3	26.6	13.7	23.7	−7.9	13.4
11	1.07	−7.7	22.6	−27.6	18.3	65.6	25.9	40.5	23.8	5.1	13.4
12	0.77	−6.7	22.2	−9.7	18.3	21.1	25.9	−18.2	24.1	2.9	13.4
13	0.46	−49.2	22.3	4.6	18.3	−70.7	26.0	−36.1	24.2	−40.7	13.4

Gaussian, the upper limits to $\Delta T/T$ derived for a Gaussian sky correlation function will be lower than those for any other assumed correlation (Silk 1993).

The four channels allowed a limited amount of spectral analysis. A best-fit signal, assumed to be a power law, $T \propto \nu^{\beta}$, was found to have a spectral index β of $-2 + 1.5, -1.75$. An identical analysis was applied to points 7 and 8, where most of the detected signal lies. The remaining 11 points defined a baseline, which we subtracted. This yielded an index of $-2.5 + 1.3, -1.5$. A thermal spectrum, expected for most CBR anisotropies, would have an index of 0 if the effects of changing beam size with increasing frequency are ignored. These effects are expected to increase the index of a thermal signal for most expected sky correlation functions.

7. DISCUSSION

Under the assumption that all of the signal is CBR anisotropy, the data yield a 95% confidence upper limit of $\Delta T/T \leq 1.6 \times 10^{-5}$. This is consistent with the previously published limit of $\Delta T/T \leq 1.4 \times 10^{-5}$ of Gaier et al. (1992). The maximum likelihood detection at $\Delta T/T = 8.6 \times 10^{-6}$ at 1°.5 is consistent with standard cold dark matter (CDM) models that are normalized at larger angles by the *COBE* DMR detection. Such scenarios (with $H_0 = 50$, $\Omega_B = 0.05$ and $n = 1$) predict anisotropy in our beam of $\Delta T/T \sim 1 \times 10^{-5}$ (Bond 1992).

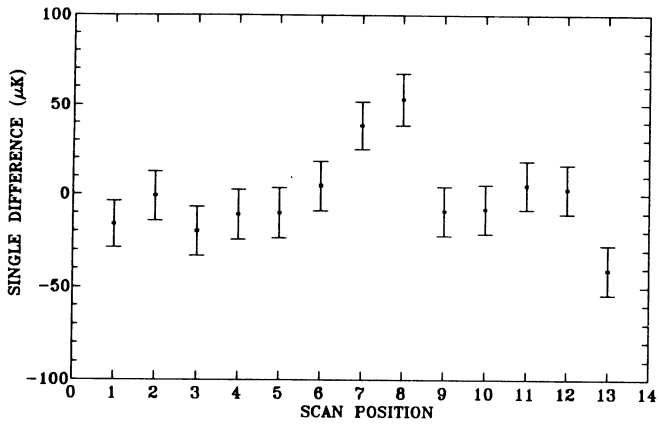

FIG. 2.—Likelihood for the full band data, normalized to the maximum value. Assumes a Gaussian correlated sky with a 1°.5 coherence angle.

The spectrum of the measured signal is unlike a CBR signal, but the data do not rule out a CBR detection at better than 2 σ. If we knew a priori that points 7 and 8 were contaminated (which we do not) and therefore remove them from the data set, a very restrictive upper limit of 8×10^{-6} is set. This upper limit would place stringent limits on most standard recombination CDM models.

8. CONCLUSION

We have presented further results of data taken at the Amundsen-Scott South Pole station. Using the high sensitivity of a HEMT amplifier and the long integration times available for Antarctic observations, we obtained an extremely sensitive data set. The 13 data points we present here set an upper limit of $\Delta T/T \leq 1.6 \times 10^{-5}$. This is consistent with previously published results from this expedition. The data show a clear detection at the level of 8.6×10^{-6}, a value consistent with CDM theories. However, identification of the source of the signal is not possible on the basis of the measured spectrum. The spectrum is more consistent with emission from electrons via free-free or synchrotron processes than it is with a CBR signal. If points 7 and 8 are hypothesized to be contaminated, and therefore removed, the result is an upper limit of $\Delta T/T \leq 8 \times 10^{-6}$.

Because we are close to being able to distinguish between the aforementioned possibilities, more data are needed, and we plan a return to the South Pole in late 1993. Work is also continuing to analyze the entire data set in the context of structure formation theories.

We would like to thank D. Bond, J. Silk, N. Vittorio, K. Gorski, and M. White for useful comments regarding the analysis process. Special thanks go out to M. Pospieszalski and M. Balister of NRAO-CDL for useful information regarding amplifiers and for supplying the outstanding HEMT amplifiers. This project would have been impossible without the support of B. Sadoulet and the Center for Particle Astrophysics. The assistance we received from B. Coughran and the entire staff of the Amundsen-Scott South Pole Station would be great under any conditions, and was especially so given the

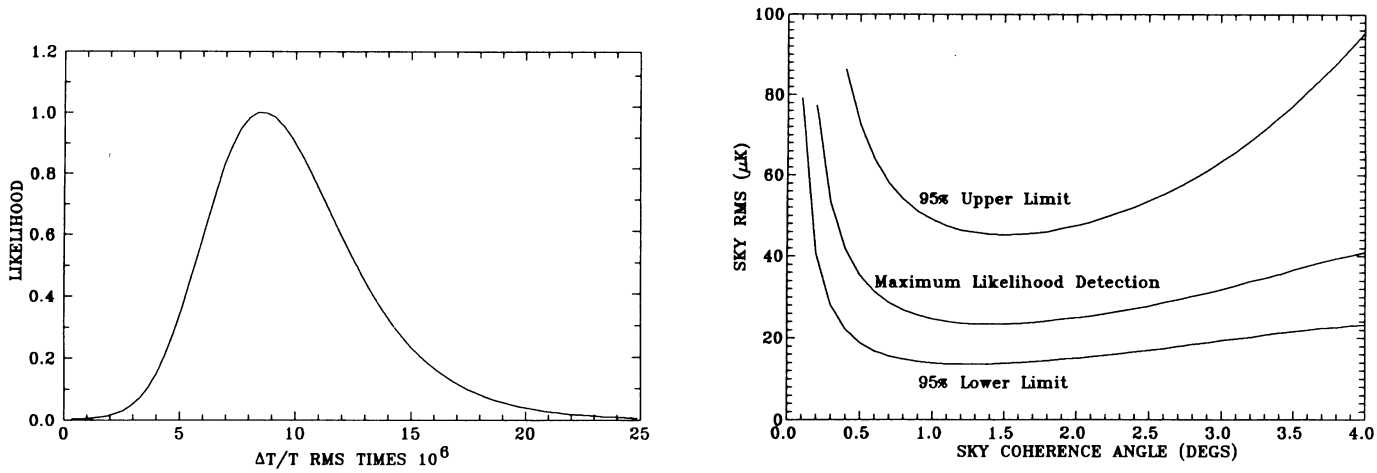

FIG. 3.—95% confidence upper limit, maximum to the likelihood, and 95% confidence lower limit, for an assumed Gaussian sky autocorrelation function

difficult working environment. This work was supported by the National Aeronautics and Space Administration under grant NAGW-1063; the National Science Foundation under polar grant NSF DPP 89-20578; and the Center for Particle Astrophysics under grant NSF UCB AST 88-0916. The work of C. A. Wuensche was partially supported by a fellowship from the Conselho Nacional de Desenvolvimento Científico e Tecnológico (CNPq) of Brazil, under 200833/91.0–CSET.

REFERENCES

Bond, J. R. 1992, private communication
Bond, J. R., & Efstathiou, G. 1987, MNRAS, 266, 655
Bond, J. R., Efstathiou, G., Lubin, P. M., & Meinhold, P. R. 1991, Phys. Rev. Lett., 66, 2179
Gaier, T., Schuster, J., Gundersen, J., Koch, T., Seiffert, M., Meinhold, P., & Lubin, P. 1992, ApJ, 398, L1
Gorski, K. 1992, ApJ, 398, L5
Meinhold, P., Chingcuanco, A., Gundersen, J., Schuster, J., Seiffert, M., Lubin P., Morris, D., & Villela, T. 1993, ApJ, 406, 12
Meinhold, P., & Lubin P. 1991, ApJ, 370, L11
Pospieszalski, M. W., Gallego, J. D., & Lakatosh, W. J. 1990, IEEE MTT-S Digest, 1253
Readhead, A. C. S., Lawrence, C. R., Myers, S. T., Sargent, W. L. W., Hardebeck, H. E., & Moffet, A. T. 1989, ApJ, 346, 566
Sachs, R. K., & Wolfe, A. M. 1966, ApJ, 147, 73
Schuster, J., Gaier, T., Gundersen, J., Meinhold, P., Koch, T., Seiffert, M., Wuensche, C. A., & Lubin, P. 1993, Ann. 16th Texas Symp./3d Symp. on Particles, Strings, and Cosmology, in press
Silk, J. 1993, private communication
Smoot, G., et al. 1992, ApJ, 396, L1
Vittorio, N., & Silk, J. 1992, ApJ, 385, L9
Wilson, M., & Silk, J. 1981, ApJ, 243, 14
Wright, E., et al. 1992, ApJ, 396, L13